Int. J. Environ. Sci. Technol. (2016) 13:1257–1268
DOI 10.1007/s13762-016-0964-9

ORIGINAL PAPER

Adsorption of aqueous Pb(II), Cu(II), Zn(II) ions by amorphous tin(VI) hydrogen phosphate: an excellent inorganic adsorbent

C. Zhu[1,3] · X. Dong[2] · Z. Chen[3] · R. Naidu[3]

Received: 18 September 2015 / Revised: 28 January 2016 / Accepted: 17 February 2016 / Published online: 7 March 2016
© Islamic Azad University (IAU) 2016

Abstract Amorphous tin(VI) hydrogen phosphate (ATHP) was synthesized using the liquid phase precipitation method and served as an adsorbent to remove Pb(II), Cu(II), and Zn(II) from aqueous solutions. The ATHP was characterized by powder X-ray diffraction (XRD), transmission electron microscopy (TEM), scanning electron microscopy (SEM), X-ray photoelectron spectroscopy (XPS), and nitrogen adsorption–desorption techniques. Adsorption properties were evaluated as a function of pH, reaction time, concentration of reactants, and salinity. Their equilibrium adsorption data were modeled using Freundlich, Langmuir, and Dubinin–Kaganer–Radushkevich isotherms, respectively. The results revealed that adsorption equilibrium reached within 180 min. ATHP indicated good adsorption even below the pH_{ZPC}, and best adsorption at pH 5 for Pb(II) and Cu(II) and at pH 5.5 for Zn(II) was observed. Equilibrium data fitted better to the Langmuir model for Pb(II) and Cu(II) and fitted better to the Freundlich model for Zn(II). The saturated adsorption capacities deduced from the Langmuir model were 2.425, 1.801, and 0.600 mmol/g for Cu(II), Pb(II), and Zn(II), respectively, indicating an adsorption affinity order of Cu > Pb > Zn. There is a negative correlation between the concentration of NaCl and adsorption capacity of ATHP, yet ATHP still exhibited excellent adsorption having an adsorption capacity of 19.35, 15.16, 6.425 mg/g when the concentration of NaCl was 0.6 mol/L. The free energy (E) was 12.33, 10.70, and 14.74 kJ/mol for Pb(II), Cu(II), and Zn(II), respectively. An adsorption mechanism based on ion exchange between heavy metal ions and H^+ in the ATHP is proposed. Furthermore, the used ATHP was regenerated by HCl solution and the adsorbent was used repeatedly.

Keywords Adsorption preference · Amorphous tin(VI) hydrogen phosphate · Potentiometric titration curve · Recyclability · Saline wastewater

Introduction

Discharge of sewage with heavy metals into the natural environment has become a major public health concern owing to its non-biodegradable and persistent nature. Potential sources of heavy metal mainly include mining industries, electroplating, battery and chemical manufacturing, tannery, fertilizer, and illegal landfills as side effects of these activities (Mubarak et al. 2013). Toxic metal ions jeopardize our health when they enter drinking water supplies and other food chains (Ali and Aboul-Enein 2006). While Pb(II), Cu(II), and Zn(II) are not the most toxic and carcinogenic heavy metals among the heavy metals, their widespread production and consumption have led to high emissions and destructive outcomes. Hence,

---

Electronic supplementary material The online version of this article (doi:10.1007/s13762-016-0964-9) contains supplementary material, which is available to authorized users.

✉ X. Dong
jessicadx1221@163.com

[1] Jiangsu Institute of Marine Resources, Lianyungang 222001, Jiangsu, People's Republic of China

[2] Engineering College of Engineer Corps, PLA University of Science and Technology, Nanjing 210007, Jiangsu, People's Republic of China

[3] Global Centre for Environmental Remediation, University of Newcastle, Callaghan, NSW 2308, Australia

research on the sequestration of Pb(II), Cu(II), and Zn(II) is still of great significance.

In order to eliminate heavy metals from polluted water, various water purification methods such as chemical precipitation, coagulation, ion exchange, electrolytic methods, membrane separation processes, and adsorption have been proposed (Wan et al. 2010; Metwally et al. 2013; Tao et al. 2014; Jamshidi Gohari et al. 2013; Gupta et al. 2012). Of these methods, adsorption is considered to be the most universal and promising water treatment and reclamation technology due to its cost-effectiveness, simplicity, and flexibility in operation, especially combined with appropriate regeneration steps (Ali 2010). Another advantage of adsorption is that there is no secondary sludge pollution, and this means not having to invest in infrastructure and sludge-related operations (Semerjian 2010). To date, numerous materials as potential adsorbents for the sequestration of hazardous heavy metals have been studied, such as bottom fly ash (Khan et al. 2009), sawdust (Semerjian 2010), peanut husk charcoal (Shang et al. 2015), clinoptilolite (Mihaly-Cozmuta et al. 2014), chemically modified orange peel (Lasheen et al. 2012), poly(amidoamine)-modified graphene oxide (Yuan et al. 2013), magnetic Fe_3O_4 functionalized with EDTA (Liu et al. 2013), and carbon nanotubes/silica nanoparticles (Saleh 2015b). Some adsorbents may be low cost, but removal efficiency is poor from a practical perspective. Some organic adsorbents may suffer from degradation or/and release into water, leading to secondary pollution. Hence, there is a need to explore novel and environmentally friendly alternatives with high adsorption capacity, especially in severe conditions.

In recent years, inorganic nanomaterials have attracted great attention in wastewater treatment (Saleh 2015a). CdS/ZnS core–shell nanoparticles (Amiri et al. 2014), layered protonated titanate nanosheets (Lin et al. 2014), hybrid $H_nPMo_{12}O_{40}$@$Fe(III)_xSn(II)_ySn(IV)_{1-x-y}$ (Yousefi et al. 2015), and MWCNT/MnO_2 (Saleh et al. 2011) have been analyzed for their ability to remove heavy metals. The literature survey suggests that inorganic nanomaterials are attractive due to their remarkable physical and chemical properties. However, there are still some issues to be solved, such as the complex preparation procedure, and they are not applicable in acidic conditions.

The phosphates of tetravalent metals, as one non-soluble inorganic salt, have many attractive properties such as high thermal stability, resistance to acid, alkalinity, oxidation, and good ion-exchange ability. Since (Clearfield and Stynes 1964) reported the synthesis of crystalline zirconium phosphate by refluxing gelatinous precursor, many studies have been done with zirconium phosphate or its derivatives in the field of novel material (Shakshooki et al. 2015), catalyst (Wen et al. 2015), photophysics (Marti et al. 2007), medical science (Deshapriya et al. 2014), and the environment (Pica et al. 2015). By contrast, not much research has focused on tin(VI) hydrogen phosphate, especially in the context of saline wastewater decontamination.

In this work, amorphous tin(VI) hydrogen phosphate (ATHP) was synthesized as an excellent alternative material for the removal of Pb(II), Cu(II), and Zn(II) in wastewater, especially in high-salinity media. The as-synthesized ATHP was characterized. Various experimental conditions such as solution pH, reaction time, initial concentration of heavy metals, and salinity were investigated. Three models, namely the Freundlich, Langmuir, and Dubinin–Kaganer–Radushkevich (D-K-R) systems, were used to fit the isothermal adsorption data. Recovery and regeneration experiments were also conducted. Subsequently, the adsorption mechanism was proposed. The work was performed at Huaihai Institute of Technology, China, during 2013–2014.

Materials and methods

Materials

Tin(IV) tetrachloride [$SnCl_4{\cdot}5H_2O$, 99.0 %], lead(II) nitrate [$Pb(NO_3)_2$, 99.99 %], copper sheet [Cu, 5 N], zinc granule [Zn, 5 N], sodium chloride [NaCl, 99.5 %], phosphoric acid [H_3PO_4, 85.0 %], hydrogen chloride [HCl, 36.0–38.0 %], nitric acid [HNO_3, 65.0–68.0 %] were purchased from Sinopharm Chemical Reagent Co. Ltd (Shanghai, China). All chemicals were of analytical grade or better and used as received without further purification. All glassware was acid washed, soaked, and water rinsed beforehand. All solutions were prepared by using ultrapure water (resistivity 18.2 MΩ cm).

Preparation of ATHP

ATHP was synthesized through the liquid phase precipitation method. In a typical procedure, 500 mL of 0.30 mol/L $SnCl_4$ and 0.60 mol/L H_3PO_4 solution was added dropwise until the P/Sn mole ratio was 4 with continuous stirring at 25 °C. The resulting white mixture was kept for 12 h in a water bath (25 °C), centrifuged, washed with conductivity water till free of chloride ions, and then vacuum dried at 60 °C. The materials obtained were sized by sieving to 160 mesh size and kept in air-tight containers for characterization and adsorption experiments.

Characterization of ATHP

N_2 adsorption and desorption experiment at 77 K was tested on a SA3100 Plus apparatus (Beckman Coulter, USA) to determine the specific surface area and pore volume. Transmission electron microscopy (TEM) image was observed on a JEM 2100F STEM microscope (JEOL, Japan) with an acceleration voltage of 200 kV. The powder samples were dispersed ultrasonically in methanol and then pre-deposited onto copper grids. Scanning electron micrograph (SEM) was obtained on a JSM-6390LA microscope (JEOL, Japan) by applying 15 kV voltage. Phase analysis was done using X-ray diffraction (XRD) on a SCINTXTRA diffractometer (ARL, Swiss) with CuK_α radiation ($\lambda = 1.54$ Å) in the range of 2θ value between 4° and 70° with a scanning speed of 2°/min.

X-ray photoelectron spectroscopy (XPS) analysis was executed using a Thermo ESCALAB 250 photoelectron spectrometer. Experiments were carried out with the standard Al$K\alpha$ radiation source ($h\nu = 1486.6$ eV, 150 W) under 2×10^{-9} mbar vacuum. The shift of the binding energy was referenced to C1s hydrocarbon carbon peak at 284.8 eV.

Potentiometric titration was carried out in an automatic potentiometric titrator (ZDJ-4A, Shanghai Precision and Scientific Instrument Corporation, China) at room temperature. In the potentiometric titration experiment, 0.1 g of ATHP was put into 50 mL of 0.1 mol/L KCl solution with the pH value pre-adjusted to 3 with 0.1 mol/L HCl or KOH. 0.1 mol/L KOH was then slowly added to the suspension from the microburette under continuous stirring until the pH value reached 9.0. For comparison, blank titration was conducted without adding ATHP.

Adsorption and desorption experiments

Adsorption experiments

The stock solutions of Pb(II), Cu(II), and Zn(II) used in the adsorption experiments were obtained by dissolving $Pb(NO_3)_2$, copper sheet, or zinc granule in nitric acid solution. A further working solution was freshly made by diluting the stock solution.

The batch adsorption experiments were carried out in a series of 250 mL Erlenmeyer flasks by adding 0.1 g of ATHP to 100 mL of Pb(II), Cu(II) or Zn(II) working solution at specific concentration (C_i) and pH adjusted with 0.2 mol/L HNO_3 or 0.2 mol/L NaOH solution. NaCl was used to adjust salinity. The flasks were agitated in a rotary and thermostatical oscillator at 120 rpm and 25 °C. The samples were collected at a predetermined time interval. The mixture was filtered and the first 30 mL filtrate abandoned. Then the residual concentration of metal ions in the supernatant was measured by atomic absorption spectroscopy (AAS) (TAS-990, PGeneral, China). All experiments were duplicated.

The amount of metal adsorbed per unit mass of ATHP (q_e, mg/g) was defined as follows:

$$q_e = \frac{(C_i - C_e)V}{w} \tag{1}$$

where C_i and C_e are the initial and equilibrium concentration (mg/L), w is the mass of ATHP (g), and V is the volume of the solution (L).

Desorption experiments

First, adsorption of Pb(II), Cu(II), and Zn(II) with ATHP was conducted in a large-scale scenario to prepare materials for further desorption. HCl was selected as eluent agent based on prior experiment. Different concentrations of HCl were mixed with dried ATHP loaded with Pb(II), Cu(II), or Zn(II) to determine the optimal eluent concentration.

Then desorption tests were done in a similar manner to the adsorption experiments. 0.2 g ATHP loaded with Pb(II), Cu(II), and Zn(II) was mixed with 50 mL eluent agent for 180 min and shaken at 120 rpm and 25 °C. The concentration of Pb(II), Cu(II), or Zn(II) in the eluent solution was measured by AAS. Once the desorption was concluded, samples were collected and dried for reusing in a new adsorption–desorption cycle. The concentration of heavy metals in this section was 50 mg/L and the volume 50 mL.

The desorption amount (q_{des}, mg/g) can be calculated as follows:

$$q_{\text{des}} = C_{\text{des}} V_{\text{elu}} \tag{2}$$

where C_{des} is the concentration of Pb(II), Cu(II), or Zn(II) in the eluent solution (mg/L), and V_{elu} is the volume of eluent solution (L).

Results and discussion

Characterization of ATHP

Figure 1 illustrates the XRD pattern of ATHP. It is evident in Fig. 1a that no apparent diffraction peaks were observed over the whole range. A broad and weak Bragg diffraction peak centered at 25° and even weaker peak between 42° and 50° indicate that ATHP ($Sn(HPO_4)_2 \cdot H_2O$) is amorphous with poor crystallinity (Velasquez et al. 2004). The amorphous nature of ATHP is also visible according to the pattern shown in the TEM image (Fig. 1c). No diffraction pattern was found in selected area electron diffraction. The lamellar structure of ATHP is composed of nano particles with mean grain size of approximately 3 nm. An

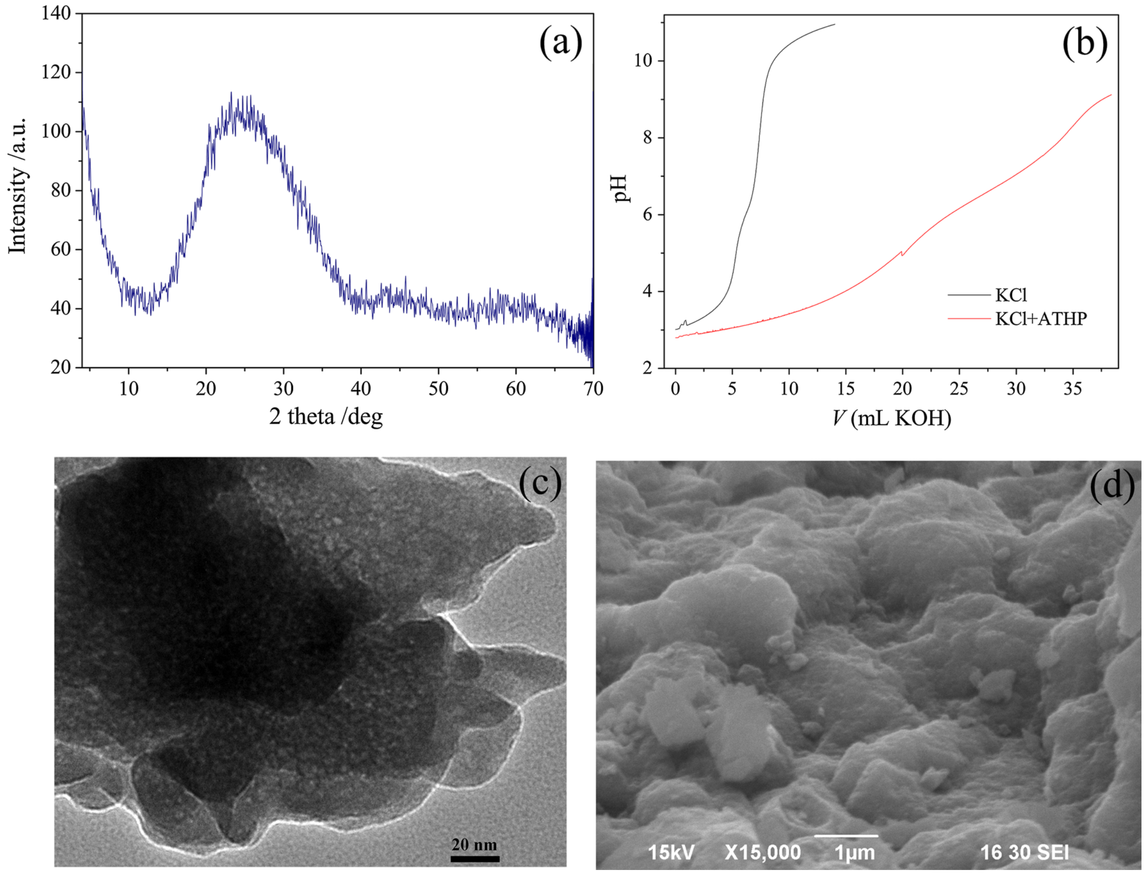

Fig. 1 **a** XRD pattern, **b** potentiometric titration curve in the media of 0.1 mol/L KCl, **c** TEM, and **d** SEM image of ATHP

observation of the SEM micrograph (Fig. 1d) indicates the presence of highly irregular pores and rough structure on the surfaces, which is favorable for adsorption. The Brunauer–Emmett–Teller (BET) specific surface area was determined as 180.9 m^2/g by N_2 adsorption–desorption method. The pore size distribution of ATHP (see Fig. S1) shows that the majority of pores fell into the range of mesopores (between 2 and 7.5 nm in diameter). The volume of BJH desorption of mesopores in this range was calculated as 0.01778 mL/g, accounting for 61.58 % of the total pore volume. This is consistent with the high porous surface revealed in the SEM image.

In order to verify the adsorption of Pb(II), Cu(II), and Zn(II) on ATHP, XPS survey spectra were scanned (see Fig. 2). The peak with binding energy of ~487 eV corresponded to Sn3d5. The peaks located around 134 and 532 eV were attributed to P2p, O1s, respectively. After the adsorption of Pb(II), Cu(II), and Zn(II), peaks at ~139, 933, and 1023.4 eV were detected, confirming the presence of Pb(4f), Cu(2p), and Zn(2p3) in the ATHP.

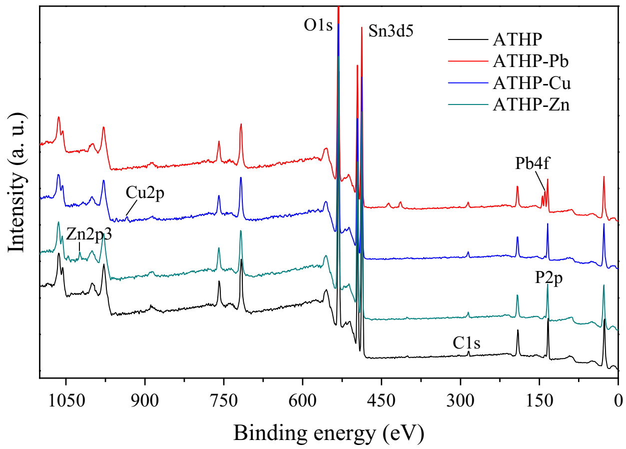

Fig. 2 XPS spectra of ATHP and ATHP loaded with Pb(II), Cu(II), and Zn(II)

Potentiometric titration curves are presented in Fig. 1b to elucidate the nature and numbers of exchangeable hydrogen ions in ATHP. The gradual increase in the suspension pH with the addition of KOH solution contrasts strikingly to the quick ascending of blank solution pH. This buffering effect confirmed the H^+ liberation from ATHP, subsequently suggesting its ion exchanging property. The two weak plateaus in the ATHP titration curve correspond to the replacement of two hydrogen ions, which signified the difference in ion exchanging ability (Parida et al. 2004). According to the chemical formula of ATHP, the theoretical ion exchange capacity is calculated as 6.08 meq/g.

Point of zero charge, defined as pH_{PZC}, refers to the electrical neutrality of the adsorbent at a particular pH value in solution (Saleh 2015a). In this study, the pH_{PZC} of ATHP was determined using the pH drift method (Chutia et al. 2009). The graph concerning final pH versus initial pH is shown in Fig. S2, and the pH_{ZPC} of ATHP was found to be 2.77.

Effect of pH

pH value is an important factor that influences the adsorption process. According to the speciation diagram (see Fig. S3), Pb(II), Cu(II), and Zn(II) exist in various species. When the pH of solution increases to 8.0, 5.9, and 7.1, precipitates of $Pb(OH)_2$, $Cu(OH)_2$, and $Zn(OH)_2$ are formed. In order to avoid metal precipitation under higher pH conditions, adsorption was carried out using pH levels of 2.5–6.0, 2.5–6.5, and 2.5–7.0 for Pb(II), Cu(II), and Zn(II), respectively. In this pH range, Pb^{2+}, Cu^{2+}, and Zn^{2+} dominate in species distribution with a declining trend in amount. Furthermore, $Pb(OH)^+$, $Cu(OH)^+$, and $Zn(OH)^+$ begin to appear at the pH of 3.1, 4.2, 6.7, respectively, with a rise in percentage. Effect of pH on the adsorption of Pb(II), Cu(II), and Zn(II) onto ATHP is depicted in Fig. 3. When the pH of the solution increased from 2.5, there was a corresponding decrease of H^+ ions in the solution and this led to an increase in deprotonation of the ATHP surface. Hence, the competition between H^+ and heavy metal ions for the binding sites on the ATHP declined while the adsorption increased. Good adsorption occurred at the pH below the pH_{ZPC} 2.77 where the net charge on the surface was positive, and this is evidence for the efficient and specific adsorption of Pb^{2+}, Cu^{2+}, and Zn^{2+}. The slight increase in adsorption at the pH higher than pH_{ZPC}, where the surface of the adsorbent was negative, was also observed. Earlier studies have reported similar patterns for the effect of pH on the adsorption of heavy metals (Momčilović et al. 2011; Akkaya 2013). It was observed the adsorption reached a plateau around pH 5.0, 5.0, and 5.5 for Pb(II), Cu(II), and Zn(II) with an adsorption amount 24.06, 19.35, and 16.3 mg/g, respectively. Therefore, all the adsorption experiments were carried out at the pH as stated previously.

It should be noted that precipitate was not found at pH 6.5 in the Cu(II) adsorption system, which may be attributed to the dynamic conversion from $Cu(OH)_2$ to $Cu(OH)^+$ and Cu^{2+} owing to the preferential removal of $Cu(OH)^+$ and Cu^{2+}. It is also worth noting that all of the pH values in each flask fell to some extent, which indicated the release of hydrogen ions while the heavy metal ions were adsorbed and this verified the ion exchanging property of ATHP.

Effect of contact time

The variation in Pb(II), Cu(II), and Zn(II) adsorption as a function of reaction time is shown in Fig. 4. Analysis of this data suggests that the adsorption was very fast in the first few minutes, slowed down thereafter, and reached equilibrium after approximately 180 min. The ratios of the adsorption amount at 10 min, equilibrium time to the maxima are 91.83, 75.81, 83.42, and 98.20, 96.69, and 99.20 % for Pb(II), Cu(II), and Zn(II), respectively. The relatively short equilibrium time (180 min) is considered to indicate a chemically controlled process, rather than a diffusion-controlled process (Horsfall and Spiff 2005).

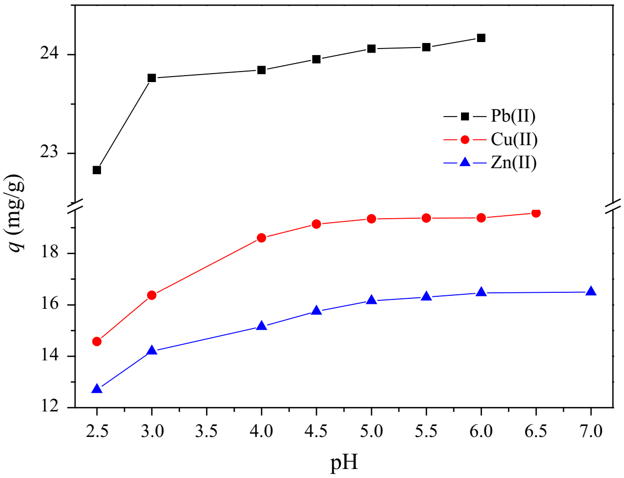

Fig. 3 Effect of pH on Pb(II), Cu(II), and Zn(II) adsorption by ATHP ($C_i = 50$ mg/L, $w = 2$ g/L, 25 °C, $t = 10$ h)

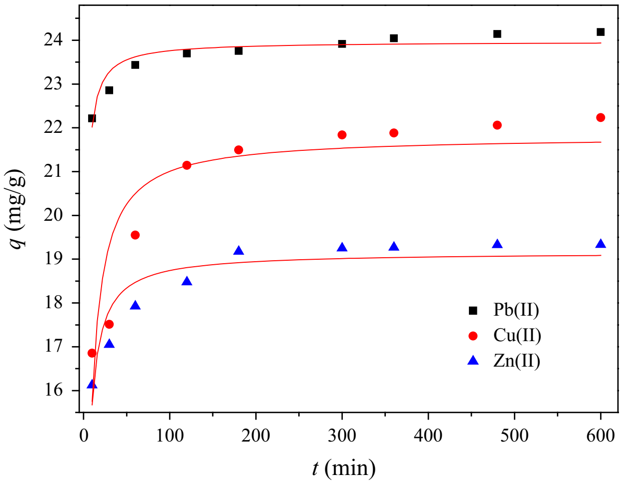

Fig. 4 Effect of reaction time on Pb(II), Cu(II), and Zn(II) adsorption by ATHP ($C_i = 50$ mg/L, $w = 2$ g/L, 25 °C, Pb, Cu pH 5.0, Zn pH 5.5)

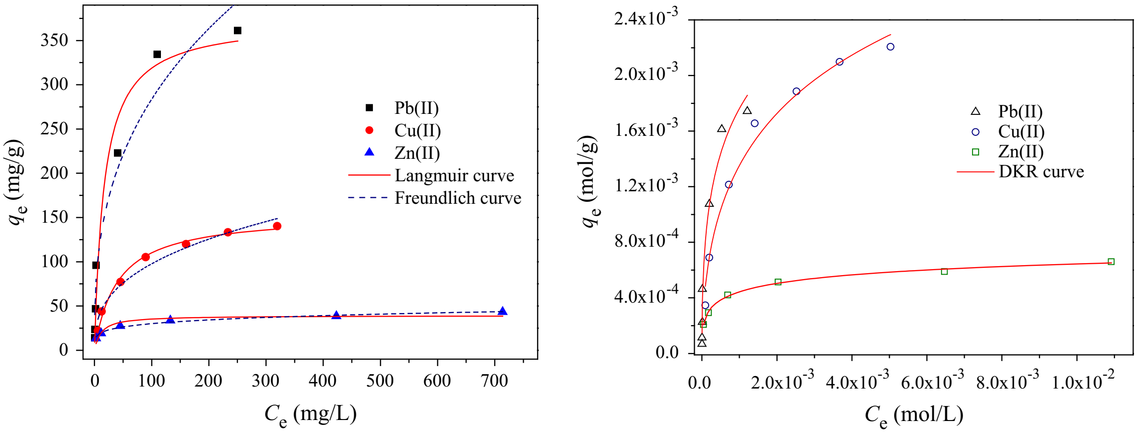

Fig. 5 Langmuir, Freundlich and D-K-R plots for adsorption of Pb(II), Cu(II), and Zn(II) by ATHP ($C_i = 30$–1000 mg/L, $w = 2$ g/L, 25 °C, 180 min, Pb(II), Cu(II) pH 5.0, Zn(II) pH 5.5)

Further extension of reaction time is not time-effective, and for this reason, 180 min was selected for further experiments.

Adsorption isotherm

The equilibrium adsorption data are useful for understanding the interaction between adsorbate and adsorbent, and to design and operate the adsorption process. Several isothermal models have been used for the data analysis. In this study, three models, i.e., Freundlich, Langmuir, and Dubinin–Kaganer–Radushkevich (D-K-R) isotherms, are employed to investigate the single-solute adsorption process.

The Freundlich isotherm is an empirical equation for adsorbents with heterogeneous surfaces and can be expressed as (Lasheen et al. 2012) follows:

$$q_e = k_F C_e^{1/n} \tag{3}$$

The Langmuir model assumes the adsorbent exhibits a homogeneous surface, and all the adsorbent sites have equal affinity to the adsorbate. The equation is described below (Lasheen et al. 2012):

$$q_e = \frac{b q_m C_e}{1 + b C_e} \tag{4}$$

where q_e (mg/g) is the adsorption capacity at equilibrium with corresponding concentration C_e (mg/L); b (L/mg) is the Langmuir constant related to the free adsorption energy; and q_m (mg/g) is the maximum adsorption capacity. k_F (mg$^{1-\mathrm{n}}$/g) and $1/n$ denote the Freundlich constant indicative of the adsorption capacity and adsorption energy, respectively.

Generally, when judging the accuracy and consistency of an isotherm model's fit to experimental equilibrium data, the magnitude of regression correlation coefficient (R) close to unity was used as the scale. However, a good R value cannot guarantee there is no bias between predictions and adsorption data, especially when the equation was linearized (Foo and Hameed 2010). Subsequently, many error functions have lately been addressed to find the best viable model that can quantify the distribution of adsorbates. In this study, Marquardt's percent standard deviation (MPSD) is used. It is similar to the geometric mean error distribution except that integrates the number of degrees of freedom. The standard deviation Δq (%) is calculated as follows (Shahmohammadi-Kalalagh and Babazadeh 2013),

$$\Delta q = \left[\sqrt{\frac{1}{p-n} \sum_{i=1}^{p} \left(\frac{q_{\exp} - q_{\mathrm{cal}}}{q_{\exp}} \right)_i^2} \right] \times 100 \tag{5}$$

where $q_{\exp}$ and q_{cal} are adsorption capacity obtained from the experiment and model, respectively, p is the number of data points, and n the number of parameters in the isotherm equation.

The Langmuir and Freundlich adsorption isotherms of the Pb(II), Cu(II), and Zn(II) ions by ATHP are shown in Fig. 5. Nonlinear least-square regression analysis with the aid of Origin software was used to obtain isotherms parameters. The results are listed in Table 1.

Examination of the data (Table 1) shows that the Langmuir equation is better for Pb(II) and Cu(II) adsorption by ATHP owing to higher regression coefficient (R) and lower standard deviation (Δq) compared to the Freundlich model. Meanwhile, the adsorption data of Zn(II) show a better fit with the Freundlich model. The n values falling in the range of 1 and 10 reveal a favorable adsorption. The q_m values of Pb(II), Cu(II), and Zn(II) from the Langmuir model are 1.801, 2.425, and 0.600 mmol/g, respectively, which suggests the adsorption affinity of Pb(II), Cu(II), and Zn(II) for ATHP following the order: Cu > Pb > Zn.

Table 1 Langmuir and Freundlich parameters for the adsorption of Pb(II), Cu(II), and Zn(II) ions by ATHP

Metal	Langmuir				Freundlich			
	q_m (mg/g)	b (L/mg)	R	Δq (%)	k_F (mg^{1-n}/g)	n	R	Δq (%)
Pb	373.25	0.05846	0.9820	30.82	54.4805	2.7918	0.9753	100.47
Cu	154.06	0.02502	0.9947	9.17	18.4918	2.7661	0.9801	27.57
Zn	39.22	0.08963	0.9218	23.62	12.5347	5.2636	0.9896	7.54

The Dubinin–Kaganer–Radushkevich (D-K-R) model is an analogue of the Langmuir one in which the assumption of homogenous or heterogeneous adsorbent surface is not necessary. The equation could be written as (Shi et al. 2015) follows:

$$q_e = q_s \exp(-B(RT\ln(1 + 1/C_e))^2) \tag{6}$$

where q_e (mol/g) is the amount adsorbed at equilibrium, q_s (mol/g) is the saturation sorption capacity, B (mol^2/kJ^2) is the activity constant related to mean free energy of adsorption, R is the universal constant, T (K) is the reaction temperature, and C_e (mol/L) is the equilibrium concentration.

The D-K-R isotherms are also plotted in Fig. 5 together with the experimental data points. The regression coefficient (R) and standard deviation (Δq) are 0.9867, 0.9916, and 0.9972 and 64.82, 18.15, and 2.75 % for Pb(II), Cu(II), and Zn(II), respectively. The mean free energy, E (kJ/mol), was calculated from the relationship $E = 1/\sqrt{2B}$ as 12.33, 10.70, and 14.74 kJ/mol for Pb(II), Cu(II), and Zn(II), respectively. In general, if the magnitude of E lies in the 8–16 kJ/mol range, the adsorption is considered to proceed via chemical ion exchange process, while the E values of 1–8 kJ/mol indicate a physical nature (Shi et al. 2015). Thus, the adsorption mechanism in our systems can be confirmed as an ion exchange process.

The adsorption capacities q_m derived from the D-K-R model are 0.00462, 0.00487, and 0.00087 mol/g for Pb(II), Cu(II), and Zn(II), respectively, which deviate quite some way from the maximum adsorption capacities q_{max} obtained from the Langmuir model. This difference may lie in the different definitions of q_{max} and q_m in the two models (Xu et al. 2008).

It should be noted that even significant fall of pH values in the equilibrium adsorption process was found. The ratio of hydrogen ions increased when M (M = Pb, Cu) was adsorbed from 2.06 to 2.14 by linear fitting (see Fig. S4), which is close to the theoretical value of 2; this demonstrates an adsorption mechanism as follows,

$$\mathrm{Sn(HPO_4)_2 + M^{2+} \rightarrow SnM(PO_4)_2 + 2H^+ (M = Pb, Cu)} \tag{*}$$

As for Zn(II), there is a poor linear relationship between the increase in hydrogen ions and Zn(II) being adsorbed (not shown). This implied the existence of a multi-mechanism except for ion exchange as listed in equation (*).

As for the difference in adsorption favorability of adsorbent for the heavy metals, this may be due to a number of influencing factors, e.g., electronegativity, hydration radii, hydration enthalpies, and solubility of the cations. Theoretically, for the ions having the same valence, the smaller ion will hold hydration water more strongly due to a higher charge density and hence larger hydration capacity resulting in weaker binding of the ion on the adsorbent (Bohli 2013). Electronegativity indicates the tendency of an atom to attract electrons. It is expected that metals with higher electronegativity will show enhanced preference (Zhang 2011). In the adsorption system of Pb, Cd, and Zn onto Fe(III)-modified zeolite, hydrate ion radii and hydration energy are deemed to be the key factors in this process (Mihajlovic et al. 2014), while the sorption affinity sequence Cu > Zn > Pb with Lewatit CNP 80 as ion exchanger shows inverse relationship with the ionic (Pehlivan and Altun 2007). Schwertmann and Taylor reported the adsorption selectivity of several transition metals for goethite followed the order of Cu > Pb > Zn > Cd > Co > Ni > Mn, which is quite consistent with electronegativity as an leading factor (Schwertmann and Taylor 1989). Therefore, we find that the adsorption preference order varies with the sort of sorbents since the interaction mechanism between adsorbates and adsorbents differs remarkably. While diverse citation sources about the chemical characteristics data of the metal ions exist, and the data sometimes are different and even contradictory, they may nonetheless contribute to this non-conformity about the relationship between the influence factors and the adsorption favorability.

Table 2 summarizes the above-mentioned characteristics of the metals used in this study. The adsorption affinity observed in this study agrees well with the magnitude of electronegativity (Cu > Pb > Zn), which echoes other studies (Wang et al. 2013; Schwertmann and Taylor 1989). The adsorption preference shows no consensus with radius, hydrated radius and hydration enthalpies. However, the correlation between the negative logarithmic values of the metal's first hydrolysis constant and maximum adsorption is observed, with a regression coefficient (R) 0.9553. It has been pointed out that a higher hydrolysis constant will lower the degree of salvation of metal ions, thus enabling them to better approach the adsorbent surface and exert better adsorption (Burns et al. 1999). This trend was also reported elsewhere (Schwertmann and Taylor 1989; Brümmer 1984; Elliott et al. 1986).

Adsorption in saline solution

Salinity plays an important role in the adsorption process because the existence of the electrolyte ions in the solution will cause changes in adsorbate activities, and adsorbent surface charge by electrostatic interactions. The comprehensive impact is negative in many circumstances. Seawater predominantly consists of about 3.5 % of sodium chloride (NaCl) which is around 0.6 mol/L. In this study, the concentration of NaCl varies from 0 to 0.7 mol/L. Figure 6a depicts the effects of salinity on the adsorption of Pb(II), Cu(II), and Zn(II) by ATHP in a single-component system. As the concentration of NaCl increases, the adsorption capacity of Pb(II), Cu(II), and Zn(II) all decreased in varying degrees. At the concentration of 0.6 mol/L, the adsorption capacity was 19.35, 15.16, and 6.425 mg/g, which was 82.43, 74.64, and 41.99 % compared with the quantity at zero NaCl for Pb(II), Cu(II), and Zn(II), respectively. Figure 6a also indicates a negative correlation between the concentration of NaCl and adsorption capacity with correlation coefficient (*R*) of 0.9389, 0.9568, and 0.9928, which may be explained by the competition of Na^+ with heavy metals for the adsorption sites, the formation of Cl^- complexes which are not adsorbable, and the decrease of available Pb^{2+}, Cu^{2+}, and Zn^{2+}.

Figure 6b shows the effect of salinity on the adsorption of Pb(II), Cu(II), and Zn(II) by ATHP in coexistence systems under varying concentrations of NaCl. Inhibition effect was observed in the multi-ions and saline system with 26.3, 46.0, and 64.6 % drop in adsorption capacity at the NaCl concentration of 0.6 mol/L compared with that shown in Fig. 6a for Pb(II), Cu(II), and Zn(II), respectively. The corresponding adsorption capacities were 14.25, 8.18, and 2.28 mg/g, which showed great superiority over the adsorbent reported (Xu et al. 2008; Green-Ruiz et al. 2008).

Desorption studies

From a practical point of view, reusability is very important for an application-oriented adsorption. Different concentrations of HCl were investigated to determine the best conditions. The desorption ratios of Pb(II), Cu(II), and Zn(II) are 91.14, 92.64, and 97.30 %, respectively, when

Table 2 Electronegativity, radius, hydration radius, and hydration heat of metal ions

Metal	Radius (Pauling's rules) (nm)[a]	Hydrated radius (nm)[a]	Hydration enthalpies (kJ/mol)[a]	Electronegativity (Pauling scale)[b]	Hydrolysis constant (pK_1)[b]
Cu	0.073	0.419	−2010	2.0	7.5
Pb	0.120	0.401	−1481	1.87	7.8
Zn	0.074	0.430	−1955	1.65	9.6

[a] (Golomeova et al. 2014)

[b] (McBride 1989)

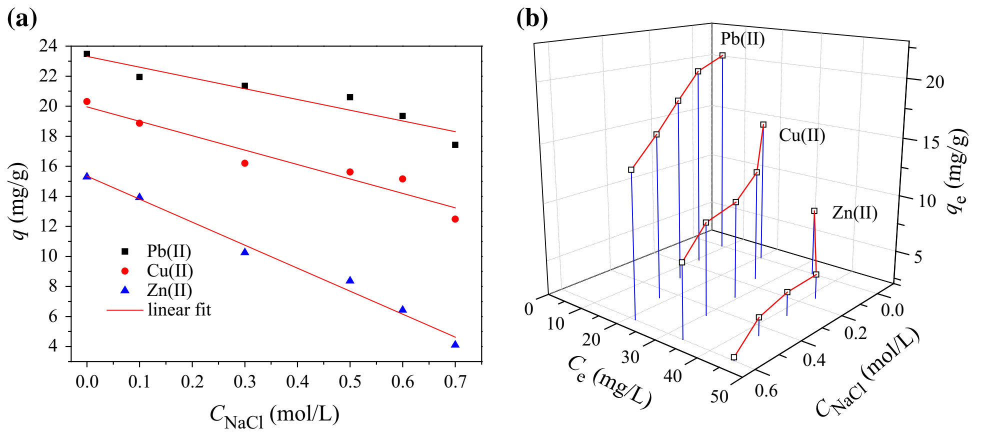

Fig. 6 Effect of salinity on the removal of Pb(II), Cu(II), and Zn(II) by ATHP **a** single-component system (C_i = 50 mg/L, c(NaCl) = 0-0.7 mol/L, *w* = 2 g/L, 25 °C, 180 min, Pb(II), Cu(II) pH 5.0, and Zn(II) pH5.5); **b** coexistence systems (C_i = 50 mg/L, c(NaCl) = 0–0.6 mol/L, *w* = 2 g/L, 25 °C, 180 min, pH 5.0)

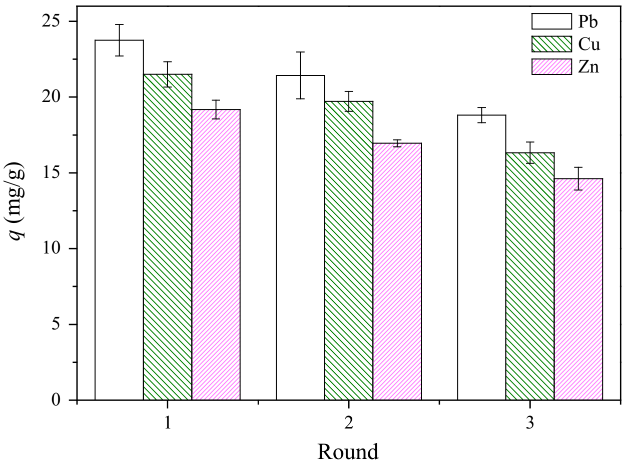

Fig. 7 Reusability of ATHP during three adsorption–desorption–regeneration cycles

the concentration of HCl is 0.5 mol/L, while the desorption ratios are 92.57, 94.79, 98.05, 95.30, 94.94, and 98.24 % when the concentrations of HCl are 3 and 5 mol/L, also, respectively. It is clear that a higher concentration of HCl favors the desorption process. However, the increase in concentration cannot lead to a significant grow in desorption amount, and therefore it is not cost-effective. So, 0.5 mol/L HCl was selected as the eluent agent for further analysis. The adsorption–desorption cycle was repeated three times in this study, and the results are shown in Fig. 7. It can be seen that the adsorption capacity in the second and third cycles decreased by approximately 10 % owing to the incomplete desorption; however, the ATHP still maintained high adsorption efficiency. The adsorption amount was maintained at 18.81, 16.33, and 14.62 mg/g for Pb(II), Cu(II), and Zn(II), respectively. These results suggest that ATHP is an effective and recyclable adsorbent for the removal of Pb(II), Cu(II), and Zn(II) in wastewater treatment.

Comparison with other adsorbents

The high adsorption ability of ATHP can be ascribed to its mesoporous structure, high specific surface, and intrinsic nature. The Sn atoms lying very nearly in a plane were bridged by O_3P-OH which had a tetrahedral structure with a P atom situated in the center. Of the four O atoms in the O_3P-OH group, three are bonded to three different Sn atoms and the fourth O atom is bonded with the H atom (Clearfield and Stynes 1964). The interconnected Sn-O-P-O-Sn structure makes these atoms very stable and will not leach out when placed in an aqueous solution. The ion exchange property lies in the hydrogen ion in P-O-H. AAS analysis in this study showing no Sn element in the reaction solution confirmed no leaching of Sn.

Table 3 summarizes the maximum adsorption capacity of ATHP and other adsorbents reported in the literature toward Pb(II), Cu(II), and/or Zn(II) removal. Most of the maximum adsorption capacities are calculated using the Langmuir isotherm. A comparison shows that ATHP is clearly superior over many adsorbents for Pb(II), Cu(II), and Zn(II) from aqueous solutions. The biggest shining spot of ATHP as a potential candidate for removing heavy metals is its inorganic nature, insolubility in water, acid and base, good thermal stability, facile preparation procedure, and low cost. However, ATHP in the form of ultrafine

Table 3 Maximum adsorption capacities of various adsorbents for Pb(II), Cu(II), and/or Zn(II) removal

Adsorbent	Adsorption capacity (mg/g)			References
	Pb(II)	Cu(II)	Zn(II)	
CSH/chitosan mesoporous microspheres	796	425	400	(Zhao et al. 2014)
Montmorillonite–kaolinite clay with TiO_2	71.1	42.9	15.4	(Đukić et al. 2015)
Amidoxime chelating resin	331.5	185.6	–	(Shaaban et al. 2014)
Graphitic-C_3N_4	281.8	133.8	–	(Shen et al. 2015)
Hydrous manganese dioxide	100.3	36.5	–	(Hasan and Jhung 2015)
S-doped graphene sponge	–	228	–	(Zhao et al. 2015)
multi-carboxyl-functionalized silica gel	–	47.07	39.96	(Li et al. 2014)
Dithiocarbamate functionalized MWCNT	–	98.1	11.2	(Li et al. 2015)
Nanoporous activated neem bark	–	21.2	11.9	(Maheshwari et al. 2015)
Commercial Diphonix	–	29.5	26.2	(Turhanen et al. 2015)
ATHP	373.25	154.06	39.22	Present work

"–" Stands for not available

particles cannot be directly used in large-scale operations. The immobilization of ATHP onto large porous particles or magnetic materials is essential, and relative research is underway.

Conclusion

The adsorption of Pb(II), Cu(II), and Zn(II) on ATHP was investigated using batch experiments. The removal of metal ions was highly efficient, and equilibrium time was observed within 180 min. Increasing pH favored the adsorption in the experimental pH range. ATHP demonstrated good adsorption capacity even below the pH_{ZPC} 2.77, and maximum adsorption occurred at 5.0 for Pb(II) and Cu(II) and at 5.5 for Zn(II); Pb(II) and Cu(II) adsorption isotherm data fitted the Langmuir isotherm better, while Zn(II) adsorption data fitted the Freundlich model better. The saturated adsorption capacities received from the Langmuir model were 1.801 mmol/g for Pb(II), 2.425 mmol/g for Cu(II), and 0.600 mmol/g for Zn(II). The order of adsorption selectivity was $Cu > Pb > Zn$. The adsorption mechanism is ion exchange between H^+ and metal ions. ATHP showed excellent ability to remove Pb(II), Cu(II), and Zn(II) in a saline medium when the adsorption capacities were 19.35, 15.16, and 6.425 mg/g, respectively, at the NaCl concentration of 0.6 mol/L. The heavy metal-loaded ATHP can be regenerated by HCl solution. The regenerability and recyclability of ATHP demonstrated it is a promising material for sequestering heavy metals in saline wastewater.

Acknowledgments This investigation was supported by the Development Foundation of Jiangsu Institute of Marine Resources (JSIMR201311) and Natural Science Foundation of the Jiangsu Higher Education Institutions of China (14KJD610001).

References

Akkaya R (2013) Removal of radioactive elements from aqueous solutions by adsorption onto polyacrylamide–expanded perlite: equilibrium, kinetic, and thermodynamic study. Desalination 321:3–8

Ali I (2010) The quest for active carbon adsorbent substitutes: inexpensive adsorbents for toxic metal ions removal from wastewater. Sep Purif Rev 39:95–171

Ali I, Aboul-Enein HY (2006) Instrumental methods in metal ions speciation: chromatography, capillary electrophoresis and electrochemistry. Taylor & Francis group, New York

Amiri O, Emadi H, Mostafa Hosseinpour-Mashkani SS, Sabet M, Rad MM (2014) Simple and surfactant free synthesis and characterization of CdS/ZnS core-shell nanoparticles and their application in the removal of heavy metals from aqueous solution. RSC Adv 4:10990–10996

Bohli T (2013) Comparative study of bivalent cationic metals adsorption Pb(II), Cd(II), Ni(II) and Cu(II) on olive stones chemically activated carbon. J Chem Eng Proc Technol 4:1000158

Brümmer GW (1984) Heavy metal species, mobility and availability in soils. In: Bernhard M, Brinckman FE, Sadler PJ (eds) The importance of chemical "speciation" in environmental processes. Springer, Berlin

Burns CA, Cass PJ, Harding IH, Crawford RJ (1999) Adsorption of aqueous heavy metals onto carbonaceous substrates. Colloids Surf A 155:63–68

Chutia P, Kato S, Kojima T, Satokawa S (2009) Arsenic adsorption from aqueous solution on synthetic zeolites. J Hazard Mater 162:440–447

Clearfield A, Stynes JA (1964) The preparation of crystalline zirconium phosphate and some observations on its ion exchange behaviour. J Inorg Nucl Chem 26:117–129

Deshapriya IK, Kim CS, Novak MJ, Kumar CV (2014) Biofunctionalization of α-zirconium phosphate nanosheets: toward rational control of enzyme loading, affinities, activities and structure retention. ACS Appl Mater Inter 6:9643–9653

Đukić AB, Kumrić KR, Vukelić NS, Dimitrijević MS, Baščarević ZD, Kurko SV, Matović LL (2015) Simultaneous removal of Pb^{2+}, Cu^{2+}, Zn^{2+} and Cd^{2+} from highly acidic solutions using mechanochemically synthesized montmorillonite–kaolinite/TiO_2 composite. Appl Clay Sci 103:20–27

Elliott HA, Liberati MR, Huang CP (1986) Competitive adsorption of heavy metals by soils. J Environ Qual 15:214–219

Foo KY, Hameed BH (2010) Insights into the modeling of adsorption isotherm systems. Chem Eng J 156:2–10

Golomeova M, Zendelska A, Blazev K, Krstev B, Golomeov B (2014) Removal of heavy metals from aqueous solution using clinoptilolite and stilbite. Int J Eng Res Technol 3:1029–1035

Green-Ruiz C, Rodriguez-Tirado V, Gomez-Gil B (2008) Cadmium and zinc removal from aqueous solutions by Bacillus jeotgali: pH, salinity and temperature effects. Bioresour Technol 99:3864–3870

Gupta VK, Ali I, Saleh TA, Nayak A, Agarwal S (2012) Chemical treatment technologies for waste-water recycling—an overview. RSC Adv 2:6380

Hasan Z, Jhung SH (2015) Removal of hazardous organics from water using metal-organic frameworks (MOFs): plausible mechanisms for selective adsorptions. J Hazard Mater 283:329–339

Horsfall M, Spiff AI (2005) Kinetics studies on the sorption of lead and cadmium ions from aqueous solutions by Caladium Bicolor (Wild cocoyam) Biomass. Bull Chem Soc Ethiop 19:89–102

Jamshidi Gohari R, Lau WJ, Matsuura T, Halakoo E, Ismailn AF (2013) Adsorptive removal of Pb(II) from aqueous solution by novel PES/HMO ultrafiltration mixed matrix membrane. Sep Purif Technol 120:59–68

Khan TA, Singh V, Ali I (2009) Sorption of Cd(II), Pb(II) and Cr(VI) from wastewater using bottom fly ash as low cost sorbent. J Environ Prot Sci 3:124–132

Lasheen MR, Ammar NS, Ibrahim HS (2012) Adsorption/desorption of Cd(II), Cu(II) and Pb(II) using chemically modified orange peel: equilibrium and kinetic studies. Solid State Sci 14:202–210

Li M, Li MY, Feng CG, Zeng QX (2014) Preparation and characterization of multi-carboxyl-functionalized silica gel for removal of Cu (II), Cd (II), Ni (II) and Zn (II) from aqueous solution. Appl Surf Sci 314:1063–1069

Li Q, Yu J, Zhou F, Jiang X (2015) Synthesis and characterization of dithiocarbamate carbon nanotubes for the removal of heavy metal ions from aqueous solutions. Colloids Surf A 482:306–314

Lin CH, Wong DSH, Lu SY (2014) Layered protonated titanate nanosheets synthesized with a simple one-step, low-temperature, urea-modulated method as an effective pollutant adsorbent. ACS Appl Mater Inter 6:16669–16678

Liu Y, Chen M, Yongmei H (2013) Study on the adsorption of Cu(II) by EDTA functionalized Fe_3O_4 magnetic nano-particles. Chem Eng J 218:46–54

Maheshwari U, Mathesan B, Gupta S (2015) Efficient adsorbent for simultaneous removal of Cu(II), Zn(II) and Cr(VI): kinetic, thermodynamics and mass transfer mechanism. Process Saf Environ Prot 98:198–210

Marti AA, Paralitici G, Maldonado L, Colón JL (2007) Photophysical characterization of methyl viologen ion-exchanged within a zirconium phosphate framework. Inorg Chim Acta 360:1535–1542

McBride MB (1989) Reactions controlling heavy metal solubility in soils. In: Stewart BA (ed) Advances in soil science. Springer, New York

Metwally SS, Ayoub RR, Aly HF (2013) Amidoximation of cyano group for chelating ion exchange of some heavy metal ions from wastewater. Sep Sci Technol 48:1830–1840

Mihajlovic M, Lazarevic S, Jankovic-Castvan I, Jokic B, Janackovic D, Petrovic R (2014) A comparative study of the removal of lead, cadmium and zinc ions from aqueous solutions by natural and Fe(III)-modified zeolite. Chem Ind Chem Eng Q 20:283–293

Mihaly-Cozmuta L, Mihaly-Cozmuta A, Peter A, Nicula C, Tutu H, Silipas D, Indrea E (2014) Adsorption of heavy metal cations by Na-clinoptilolite: equilibrium and selectivity studies. J Environ Manage 137:69–80

Momčilović M, Purenović M, Bojić A, Zarubica A, Ranđelović M (2011) Removal of lead(II) ions from aqueous solutions by adsorption onto pine cone activated carbon. Desalination 276:53–59

Mubarak NM, Sahu JN, Abdullah EC, Jayakumar NS (2013) Removal of heavy metals from wastewater using carbon nanotubes. Sep Purif Rev 43:311–338

Parida KM, Sahu BB, Das DP (2004) A comparative study on textural characterization: cation-exchange and sorption properties of crystalline α-zirconium(IV), tin(IV), and titanium(IV) phosphates. J Colloid Interface Sci 270:436–445

Pehlivan E, Altun T (2007) Ion-exchange of Pb^{2+}, Cu^{2+}, Zn^{2+}, Cd^{2+}, and Ni^{2+} ions from aqueous solution by Lewatit CNP 80. J Hazard Mater 140:299–307

Pica M, Nocchetti M, Ridolfi B, Donnadio A, Costantino F, Gentili PL, Casciola M (2015) Nanosized zirconium phosphate/AgCl composite materials: a new synergy for efficient photocatalytic degradation of organic dye pollutants. J Mater Chem A 3:5525–5534

Saleh TA (2015) Isotherm, kinetic, and thermodynamic studies on Hg(II) adsorption from aqueous solution by silica- multiwall carbon nanotubes. Environ Sci Pollut Res Int 22:16721–16731

Saleh TA (2015b) Nanocomposite of carbon nanotubes/silica nanoparticles and their use for adsorption of Pb(II): from surface properties to sorption mechanism. Desalin Water Treat 57:1–15

Saleh TA, Agarwal S, Gupta VK (2011) Synthesis of MWCNT/MnO_2 and their application for simultaneous oxidation of arsenite and sorption of arsenate. Appl Catal B 106:46–53

Schwertmann U, Taylor RM (1989) Iron oxides. In: Dixon JB, Weed SR (eds) Minerals in soil environments. 2nd ed. Soil science society of America, Madison, Wisconsin

Semerjian L (2010) Equilibrium and kinetics of cadmium adsorption from aqueous solutions using untreated *Pinus halepensis* sawdust. J Hazard Mater 173:236–242

Shaaban AF, Fadel DA, Mahmoud AA, Elkomy MA, Elbahy SM (2014) Synthesis of a new chelating resin bearing amidoxime group for adsorption of Cu(II), Ni(II) and Pb(II) by batch and fixed-bed column methods. J Environ Chem Eng 2:632–641

Shahmohammadi-Kalalagh S, Babazadeh H (2013) Isotherms for the sorption of zinc and copper onto kaolinite: comparison of various error functions. Int J Environ Sci Technol 11:111–118

Shakshooki SK, El-Akari FA, Jangher AA, Hamasi AM (2015) Facile synthesis of γ-Zirconium phosphate-fibrous cerium phosphate/emeraldine salt nanocomposite membrane. Am J Chem 5:75–85

Shang H, Lu Y, Zhao F, Chao C, Zhang B, Zhang H (2015) Preparing high surface area porous carbon from biomass by carbonization in a molten salt medium. RSC Adv 5:75728–75734

Shen C, Chen C, Wen T, Zhao Z, Wang X, Xu A (2015) Superior adsorption capacity of g-C_3N_4 for heavy metal ions from aqueous solutions. J Colloid Interface Sci 456:7–14

Shi J, Fang Z, Zhao Z, Sun T, Liang Z (2015) Comparative study on Pb(II), Cu(II), and Co(II) ions adsorption from aqueous solutions by arborvitae leaves. Desalin Water Treat 57:1–8

Tao H-C, Lei T, Shi G, Sun X-N, Wei X-Y, Zhang L-J, Wu W-M (2014) Removal of heavy metals from fly ash leachate using combined bioelectrochemical systems and electrolysis. J Hazard Mater 264:1–7

Turhanen PA, Vepsalainen JJ, Peraniemi S (2015) Advanced material and approach for metal ions removal from aqueous solutions. Sci Rep 5:8992

Velasquez C, Rojas F, Lara VH, Campero A (2004) On the textural and morphological properties of crystalline and amorphous α-tin phosphate. Phys Chem Chem Phys 6:4714–4721

Wan M-W, Kan C-C, Rogel BD, Dalida MLP (2010) Adsorption of copper (II) and lead (II) ions from aqueous solution on chitosan-coated sand. Carbohydr Polym 80:891–899

Wang X, Cai W, Liu S, Wang G, Wu Z, Zhao H (2013) ZnO hollow microspheres with exposed porous nanosheets surface: structurally enhanced adsorption towards heavy metal ions. Colloid Surfaces A 422:199–205

Wen M, Mori K, Kuwahara Y, Yamashita H (2015) Visible-light-responsive carbon dioxide reduction system: rhenium complex intercalated into a zirconium phosphate layered matrix. Chem Cat Chem 7:3519–3525

Xu D, Tan XL, Chen CL, Wang XK (2008) Adsorption of Pb(II) from aqueous solution to MX-80 bentonite: effect of pH, ionic strength, foreign ions and temperature. Appl Clay Sci 41:37–46

Yousefi T, Yavarpour S, Mousavi SH, Torab-Mostaedi M, Davarkhah R, Mobtaker HG (2015) Effective removal of Ce(III) and Pb(II) by new hybrid nano-material: $H_nPMo_{12}O_{40}$@Fe(III)$_x$Sn(II)$_y$-Sn(IV)$_{1-x-y}$. Process Saf Environ Prot 98:211–220

Yuan Y, Zhang G, Li Y, Zhang G, Zhang F, Fan X (2013) Poly(amidoamine) modified graphene oxide as an efficient adsorbent for heavy metal ions. Polym Chem 4:2164–2167

Zhang M (2011) Adsorption study of Pb(II), Cu(II) and Zn(II) from simulated acid mine drainage using dairy manure compost. Chem Eng J 172:361–368

Zhao J, Zhu YJ, Wu J, Zheng JQ, Zhao XY, Lu BQ, Chen F (2014) Chitosan-coated mesoporous microspheres of calcium silicate hydrate: environmentally friendly synthesis and application as a highly efficient adsorbent for heavy metal ions. J Colloid Interf Sci 418:208–215

Zhao L, Yu B, Xue F, Xie J, Zhang X, Wu R, Wang R, Hu Z, Yang ST, Luo J (2015) Facile hydrothermal preparation of recyclable S-doped graphene sponge for Cu^{2+} adsorption. J Hazard Mater 286:449–456